2020 IMEKO TC-4 International Conference on
Metrology for Archaeology and Cultural Heritage
Trento, Italy, October 22-24, 2020

DIFFERENCES BETWEEN ARCHAEOLOGICAL AND FORENSIC BURNED SAMPLES USING POWDER X-RAY DIFFRACTION (XRD) AND ATR-IR SPECTROMETRY.

Giampaolo Piga[1], Fabio Cavalli[2], Dario Innocenti[2], Eugénia Cunha[1], Stefano Enzo[3], David Gonçalves[1,4,5].

[1] *Laboratory of Forensic Anthropology, Centre for Functional Ecology, Department of Life Sciences, University of Coimbra (Portugal). giapiga@uniss.it; genac62@gmail.com; davidmiguelgoncalves@gmail.com*
[2] *Research Unit of Paleoradiology and Allied Sciences, Julian-Isontine Universitary Integrated Health Enterprise (ASUGI), Trieste (Italy). fabio.cavalli@asugi.sanita.fvg.it; dario.inox@gmail.com*
[3] *Department of Chemistry and Pharmacy, University of Sassari (Italy). enzo@uniss.it*
[4]*Archaeosciences Laboratory, Directorate General for Cultural Heritage (LARC/CIBIO/InBIO), Lisbon (Portugal).*
[5]*Research Centre for Anthropology and Health (CIAS), Department of Life Sciences, University of Coimbra (Portugal).*

***Abstract*- In this study, 105 human samples (46 crematoriums, 37 from controlled experiments and 22 archaeological cremations) were analyzed using X-ray diffraction (XRD) and infrared spectroscopy in attenuated total reflectance (ATR-IR) to highlight possible chemico- physical differences, in terms of mineralogical phases, crystallinity and spectral properties.**

I. INTRODUCTION

Requests for analysis and research on burned bones are increasingly becoming more frequent both in the archaeological and forensic fields. There are numerous investigations that can be carried out on burned bones through morphological, colorimetric-chromatic, biochemical (DNA and protein analysis) chemical and physical (for example, spectroscopic, diffractometric and radiological) methods. Besides the common problem related to fragmentation and deformation, the mechanical reduction of bone into ash of sub-millimeter dimensions is also problematic since it does not allow macroscopic morphological investigations on which burned bone analyzes are based.

To develop methods to retrieve information from material reduced to ashes, chemical and physical methodological research is increasingly being developed [1,2].

All these methods contribute to varying degrees (and depending on whether we are faced with studies of ancient populations or forensic cases) in the reconstruction of the biological profile, the state of health, the rituals and the biocultural and economic aspects.

Methodological research relating to burned bone material is based on observations of experimentally burns in muffle furnaces [3,4], in open-air fires [5], in pyres or in specially made ovens [6], of bones and teeth (intact or fragmented, with or without soft tissues) of fauna or humans (in this case, it often comes from cemetery or archaeological material, defined as "dry" with different physical characteristics compared to fresh bone, including the lower elasticity due to the difference in water content), and of animal carcasses [7].

These researches highlighted the complexity of the cremations of human bodies, influenced by various pre-combustion factors and linked to the technical characteristics of the ovens and, therefore, of the fire (duration, temperature variations, quantity of oxygen), making the heat exposure different for quality and appearance [8].

Experiments in controlled environments can highlight some qualitative aspects and contribute to understanding the causes and effects of the variables, but nevertheless they have the limitation of not always being able to return reliable quantitative values, as they do not replicate all variables that come into play in the combustion process.

The observation of commercial crematorium samples and archaeological cremations are therefore complementary to controlled experiments.

This work intends to explore the potential of ATR-IR

and XRD for a comparative study between samples that have undergone different cremations (commercial, laboratory and archaeological cremation).

II. MATERIALS AND METHODS

Forty six samples, consisting of small femoral midshaft fragments, were obtained at the end of a series of human cremations in the commercial crematorium of Trieste (Italy).

The recent samples were taken from three different skeletons of the 21st Century Identified Skeletal Collection housed at the Laboratory of Forensic Anthropology c/o Department of Life Sciences, University of Coimbra (Portugal) [9]. The first skeleton (*CEI/XXI/160*) is from an individual whose sex and age at death is known (Male; 87 years old). The remaining two skeletons (*CC/NI/17* and *CC/NI/18*) are from unidentified individuals but anthropological examinations profiled them as adult females. The burned samples comprised 19 specimens from *CEI/XXI*/160, 8 specimens from *CC/NI/17*, and 10 specimens from *CC/NI/18*.

The burned archaeological remains come from a Phoenician grave (so-called: *T250*) belonging to the Necropolis of *Monte Sirai* (Carbonia, Sardinia, Italy). The *T250* samples comprised the skull, maxilla, mandible, left (M1) and right (M1, M3) metacarpal bones, left clavicle, left and right humer, left and right ulnae, right radius, right rib 4th, left hip bone, left and right femur, right tibia, left fibula, left metatarsal 1 (MT1) and three dental fragments (13, 26 and 33 according to the ISO System).

A small fraction (~0.90 mg) of powdered bone was deposited in a dedicated sample holder for XRD analysis with a circular cavity of 25 mm in diameter and 0.5 mm in depth. The XRD patterns were collected using Bruker D2-Phaser instrument.

The Bruker D2 generator was working at a power of 30 Kv and 10 ma in the Bragg–Brentano vertical alignment with a Cu–Ka tube emission (λ = 1.5418 Å).

The width of divergent and antiscatter slits was 1 mm (0.61°). Primary and secondary axial Soller slits of 2.5° were also mounted with a linear detector LYNXEYE with 5° opening and a monochromatisation by Ni foil for the Kβ radiation. FT–IR spectra were collected in ATR mode with a Bruker Alpha Platinum-ATR interferometer in terms of absorbance vs wavenumber ν in the range 370–4000 cm^{-1}, with a resolution of 4 cm^{-1}. Each spectrum was obtained by averaging 512 interferograms. The loose powder was dispersed inside a hole cavity of spheroidal shape with its surface aligned to the plate defining it.

III. RESULTS AND CONCLUSIVE REMARKS

Careful scrutiny of XRD patterns carried out to inspect the bone structure from the crematoria suggested that a better description of the unit cell of bioapatite structure can be retrieved using a monoclinic $P2_1/c$ (n. 14 in IT) space group (S. G.) rather than the commonly adopted approximant of hydroxylapatite,beingthis latter hexagonal, space group $P6_3/m$ (n. 176 in IT). This accustoms to the believe that monoclinic form of apatited could mainly occur at high temperature [10]. Of course, it is not easy to distinguish between the two forms because of the close morphological relationships existing between the lattice parameters of the two polymorphs, i.e., $\beta_M \approx \gamma_H = 120°$; $b_M \approx 2 \cdot a_M \approx 2 \cdot a_H$ and $V_{c,M} \approx 2V_{c,H}$.

In our experience, apart from a slight but appreciable improvement of the relative difference of numerical index R_{wp} [11] in selecting the $P2_1/c$ SG rather than the $P6_3/m$ structure, significant features favouring one structure with respect to the other can be drawn by making reference to the sequence of the most intense peaks displayed in the 2θ range 30.5°-36.5° and 46.0°-58.0° as shown in the figure 1 and 2, respectively.

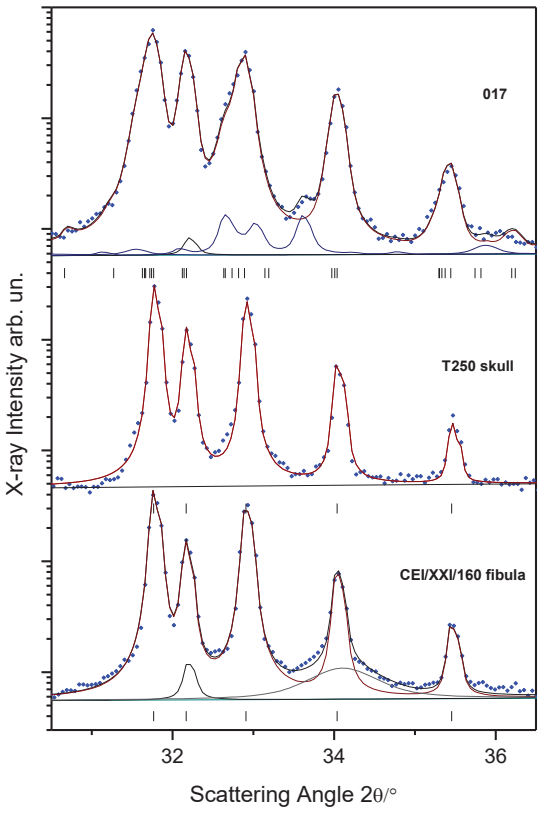

Fig. 1. A comparison of the Rietveld fit obtained from three bone specimens illustrating the different intrinsic structure description involved. Dots are from experiment, full lines refers to scattering contributions from phases found in the samples while the bars at the bottom of curves are marking the expected position of peaks.

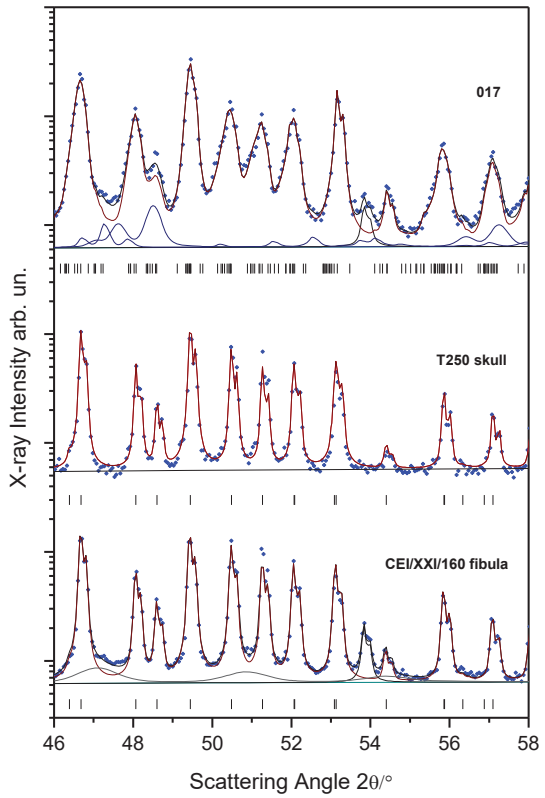

Fig. 2. Same as in Fig. 1 but referred to another portion of the reciprocal spece accessed with the experiment.

XRD patterns were were numerically refined using MAUD programme [12].
In the case of the $P6_3/m$ S. G., the sequence of zoomed peaks displayed in correspondence of the bottom bars, marking the expected occurrence of each profile, can be described in the Rietveld approach with the α_1-α_2 doublet convoluted with the mostly symmetric instrument broadening and sample broadening functions (see: *CEI/XXI/160 fibula* and *T250 skull* patterns).
Conversely, for the pattern of *017* sample, subjected to thermal treatment in commercial crematorium and reported at the top of the figure 1 and 2, respectively, it is evident the unconventional peak shape with a skeweness to the low angle side, particularly for the peaks occurring at 31.8°, 32.9° and 35.4°.
Such deformed shape can be described successfully with the contribution of several d-spacings (see bar sequence below the top patterns), possible in reason of the lowered symmetry occurring with the monoclinic description of the unit cell.
We report in the following figures 3 and 4 respectively, the arrangement of the hexagonal and monoclinic unit cell in terms of polyhedral connections, respectively [13].
We report in the following figures 3 and 4 respectively, the arrangement of the hexagonal and monoclinic unit cell in terms of polyhedral connections, respectively.

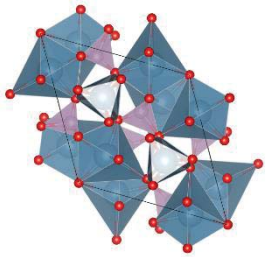

Fig. 3. The unit cell representation of hexagonal apatite projected into the a-b plane. It can be seen that P atoms are tetra-coordinated by O, sharing corners with octahedra surrounding Ca atoms. The Ca-O and P-O interatomic distances are allowed to vary according to the symmetry site.

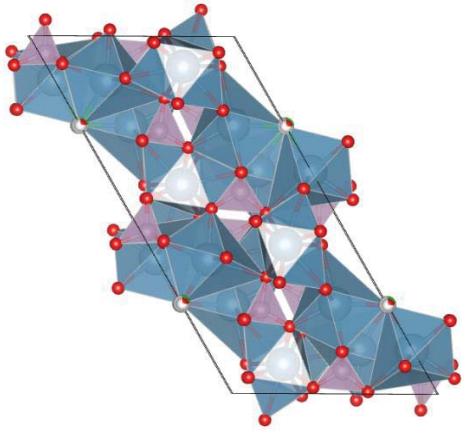

Fig. 4. Unit cell representation for the monoclinic apatite form, which was found more flexible to describe the powder patterns collected on crematoria bones. This unit cell can be obtained from two hexagonal cells piled along the b- direction and removing the restrictions to site symmetry to account appropriately for the experiment.

It can be noted that the loss of symmetry in going from the #178 S.G. to the #14 S.G. out of a scale going progressively from 1 to 230, does not correspond directly to the asymmetry observed in some peaks, being the two concepts referred to real and reciprocal space, respectively. It goes without saying that such symmetry deterioration is effected according to the specific combustive and thermal treatments carried out in the bones throughout the crematorium protocols adopted.
In fact, provided that β angle remains close to 120°, the lattice parameter ratio 2a/b can be taken as a first definition of asymmetry in the real space. Within this frame lattice, it is possible that some bond lengths of Ca-O and P-O as well as ca-P may change their value

on grounds of the lowered symmetry. This in turn is expected to show some counter effects in the spectroscopic band shape and position in the relevant ATR-IR spectra. This correlation analysis in only at a very preliminary stage and should be supported by an evaluation of the pair interatomic distance distribution to extract reliably from the final Rietveld fit data.

We can anticipate here some peculiarities extracted from the XRD pattern collection here investigated. In addition to bioapatite, four crystallographic phases were found in the crematorium samples: buchwaldite [$NaCa(PO_4)$], portlandite [$Ca(OH)_2$], calcite ($CaCO_3$), calcium oxide (CaO).

In recent burned skeletons, the presence of portlandite, β-TCP [$Ca_3(PO_4)_2$], calcite and calcium oxide was detected. Insome emblematic cases (e.g: *CC/NI/17 ulna*, *CC/NI/17 fibula* and *CC/NI/17 vertebra IV*), the bioapatite was partially transformed into β-TCP after the heat treatment at 1050° C.

In both categories of samples, a marginal decomposition of bioapatite (always > 86 wt.%) was observed, except for the rare cases described above. There are also cases in which the bioapatite, despite the high temperature they were submitted to, did not decomposed into other mineralogical phases (*CEI XXI-160 humerus distal*, *CEI XXI-160 rib 6th anterior distal*, *CC/NI/18 Vertebra I*, *CC/NI/18 Vertebra II* and *CC/NI/18 Vertebra III*).

The mineralogical phases found by the XRD analysis in archaeological T250 burned samples reveal an association of bioapatite with muscovite and calcite, mainly of diageneticorigin.

Through ATR-IR technique even more marked differences were found in the crematorium samples compared to the others, in detail:

- In all samples, the band at 562 cm^{-1} was located in the range 568-572cm^{-1}.
- In all samples, the 1022 cm^{-1} band was located at 1030 cm^{-1}, and overlapped the 1040 cm^{-1} band.
- 33 out of 46 samples show a peak (at 3642 cm^{-1}), related to the stretching mode of O-H present in calcium hydroxide [$Ca(OH)_2$] [10].

REFERENCES

[1] M.W.Warren, A.B.Falsetti, I.I.Kravchenko, F.E.Dunnam, H.A.Van Rinsvelt, W.R.Maples, “Elemental analysis of bone: proton-induced X-ray emission testing in forensic cases”, Forensic Sci Int, vol. 125, n°1, 2002, pp.37–41.

[2] T.R.Brooks, T.E.Bodkin, G.E.Potts, S.A.Smullen, “Elemental analysis of human cremainsusing ICP-OES to classify legitimate and contaminated cremains”, J Forensic Sci, vol. 51, n°5, 2006, pp. 967– 973.

[3] I.Théry-Parisot, S.Costamagno, “Propriétés combustibles des ossements: données expérimentales et réflexions archéologiques sur leur emploi dans les sites paléolithiques”, in Gallia préhistoire, 47, 2005, pp 235- 254.

[4] P.L.Walker, K.W.P.Miller, R.Richman, “Time, temperature, and oxigen availability: an experimental study of the effects of environmental conditions on the color and organic content of cremated bone” in “The analysis of burned human remains” by Schmidt C.W., Symes S.A., AP-Elsevier, 2008, pp 129-135.

[5] E.J.Pope, M.A.O’Brian, C.Smith, “Identification of Traumatic Injury in Burned Cranial Bone: An Experimental Approach”, J Forensic Sci, vol. 49 n°3, 2004, pp. 431-440.

[6] J.D.De Haan, S.J.Campbell, S.Nurbakhsh, “Combustion of animal fat and its implications for the consumption of human bodies in fires”, Sci. Justice, vol. 39, 1999, pp. 27-38.

[7] De Haan J.D., Nurbakhsh S., “Substained Combustion of an Animal Carcass and Its Implications for the Consumption of Human Bodies in Fires”, J Forensic Sci, vol. 46, n°5, 2001, pp 1076-1081.

[8] S.E.May, 2011, “The Effects of Body Mass on Cremation Weight” J Forensic Sci, January 2011, Vol. 56, n° 1, pp 3-9.

[9] M.T.Ferreira, R.Vicente, D.Navega, D.Gonçalves, F.Curate, E.Cunha, “A new forensic collection housed at the University of Coimbra, Portugal: the 21st Century Identified Skeletal Collection”, Forensic Sci Int, vol. 245, 2014, 202.e1-202.e5.

[10] M.Khachani, A.El Hamidi, M.Halim, S.Arsalane, “Non-isothermal kinetic and thermodynamic studies of the dehydroxylation process of synthetic calcium hydroxide $Ca(OH)_2$”, J. Mater. Environ. Sci vol. 5, n°2, 2014, pp. 61-64.

[11] R.A.Young, “The Rietveld Method”, IUCr Monographs in Crystallography, 5, International Union of Crystallography, Oxford University Press, New York, NY, (1993).

[12] L.Lutterotti, H.Pillière, C.Fontugne, P.Boullay, D.Chateigner, “Full-profile search–match by the Rietveld method”, J. Appl. Cryst. 52, (2019), pp. 587-598.

[13] K. Momma and F. Izumi, "VESTA 3 for three-

dimensional visualization of crystal, volumetric and morphology data," J. Appl. Cryst. 44, (2011), pp. 1272-1276.

[14] Y. El Mendili, A.Vaitkus, A.Merkys, S.Gražulis, D.Chategner, F.Mathevet, S.Gascoin, S.Petit, J.F.Bardeau, M.Zanatta, M.Secchi, G.Mariotto, A.Kumar, M.Cassetta, L.Lutterotti, E.Borovin, B.Orberger, P.Simon, B.Hehlen, M.Le Guen, "Raman Open Database: first interconnected Raman–X-ray diffraction open-access resource for material identification",J. Appl. Cryst. 52 (2019), pp. 618-625.

[15] M.Khachani, A.ElHamidi, M.Halim, S.Arsalane, "Non-isothermal kinetic and thermodynamic studies of the dehydroxylation process of synthetic calcium hydroxide $Ca(OH)_2$", J. Mater. Environ. Sci vol. 5, n°2, 2014, pp. 615-624.